Int. J. Heat Mass Transfer Vol. 25, No. 12, pp. 1857–1868, 1982
Printed in Great Britain

0017-9310/82/121857-12 $03.00/0

VISUALIZATION OF HEAT TRANSFER FROM ARRAYS OF IMPINGING JETS

R. J. GOLDSTEIN and J. F. TIMMERS
Department of Mechanical Engineering, University of Minnesota, Minneapolis, MN 55455, U.S.A.

(*Received* 25 *March* 1981 *and in final form* 20 *April* 1982)

Abstract—A visualization technique is used to measure the heat transfer coefficient distribution on a flat plate on which either a single jet or an array of jets impinges. Liquid crystals coated on a mylar sheet are used to locate isotherms on a heated surface. By adjusting the surface heat flux, contours of constant heat transfer coefficient are obtained.

NOMENCLATURE

- D, diameter of jet at exit;
- h, local heat transfer coefficient, $q_c/(T_w - T_{jr})$;
- k, thermal conductivity of fluid;
- L, jet-orifice-to-wall spacing;
- Nu, local Nusselt number, hD/k;
- q, heat flow per unit area and time;
- q_c, convective heat flux to fluid;
- q_e, electric power input per unit surface area of plate;
- q_l, energy loss per unit time and surface area of plate;
- R, radial distance from geometric stagnation point of jet (usually taken along a horizontal line);
- Re_j, Reynolds number based on velocity at jet exit, $U_j D/\nu$;
- T, temperature;
- T_{jr}, jet recovery temperature on plate;
- T_w, temperature at wall;
- U, velocity of fluid;
- U_j, average jet velocity based on orifice diameter;
- X, distance from geometric stagnation point of jet measured along wall (in vertical direction) through center of jets in 3-jet array.

Greek symbols

- ν, kinematic viscosity of fluid.

Subscript

- gb, value of parameter at green–blue boundary on liquid crystal.

INTRODUCTION

IN MANY heat and mass transfer systems including the annealing of glass sheets, the cooling of turbine blades, and the drying of paper and films, an array of impinging jets is used. The high heat and/or mass transfer in the impingement regions of the jets produces high local transport coefficients.

The heat transfer from a flat plate to a single jet has been studied [1–5]. The heat (or mass) transfer from a surface on which an array of jets impinged has also been measured [1, 6–8].

Liquid crystals have been used in several heat transfer studies. Raad and Myers [9] observed nucleation sites with pool boiling and Cooper and Petrovic [10] studied the temperature field produced by a resistively-heated cryoprobe. Hirata, Kasagi and Kumada [11] measured the surface temperature on a film-cooled wall. Klein [12] located the region of laminar–turbulent transition of the boundary layer on wind-tunnel aircraft models, but difficulties were encountered due to surface contamination, u.v. light, and flow-induced shear stress produced on the unencapsulated liquid crystals. Cooper, Field and Meyer [13] observed boundary layer transition and separation on a heated cylinder in a crossflow as well as the variation of the Nusselt number on the cylinder. Hoogendoorn and den Ouden [5] determined the local heat transfer coefficient to an impinging jet from a heated surface. The surface was heated from behind by a water bath, and the heat flux was varied by adjusting the water temperature.

In the present study, jets impinge on a heated surface. Use of an encapsulated liquid crystal permits the visualization of lines of constant temperature. With a constant heat flux boundary condition these isotherms translate into lines of constant heat transfer coefficient. Varying the magnitude of the heat flux and observing only a single isotherm results in a series of curves which provide contours of constant heat transfer coefficient on the surface.

LIQUID CRYSTALS

The liquid crystal state is an intermediate phase, a mesophase, which can occur between the solid (crystalline) state and the liquid (isotropic) state [14–16]. This intermediate phase is characteristic for certain organic compounds. In this mesophase the molecules are moveable but still ordered. There are three different kinds of mesophase: the smectic; the nematic; and the cholesteric.

A cholesteric liquid crystal system can respond to changes in temperature by sequentially passing

through the complete visual spectrum. As the temperature of a thin layer of such a liquid crystal is increased from the limiting (melting) temperature of the solid, the layer reflects mainly red light from incoming white light. As the temperature is increased further, the reflected light can change color (orange–yellow–green) until it becomes blue. At higher temperatures, the layer is fluid and, as in the solid state, transparent. It then shows the background color (usually black).

The change of color is reversible. Depending on the liquid crystal used, the color changes occur at different temperatures. Compounds have been reported covering the range from -40 to 285°C [15]. Other characteristics of liquid crystals are their generally high resolution (~ 40 lines mm^{-1}) [14] and their low heat capacity in the layer thicknesses commonly used.

THE TEST APPARATUS

A sketch of the test apparatus is shown in Fig. 1. The air flow supplied by a building compressor is smoothed, regulated, and measured before it enters the plenum. Here it is divided among the number of jets to be used in the particular test to be conducted. Each jet is formed by an individual orifice on the plate. Three different jet arrays were used: a single jet; a row of 3 jets; and an array of a single jet surrounded by a (hexagonal) set of 6 jets. These jets came from an orifice plate [8] which contains staggered rows of jet orifices. The distance between the center jet and each of its neighboring jets is four diameters ($D = 10$ mm).

The jets impinge upon a 25.4 μm thick stainless steel foil which is heated by passing an AC current through it to produce a boundary condition of approximately constant heat flux. A liquid crystal embedded on a mylar sheet is glued on the opposite side of the heating foil with a spray glue. (The encapsulated liquid crystal used was obtained from the Edmund Scientific Company, Cat. No. 72,373). The working range of the liquid crystal is 30–35°C. To minimize the heat loss, a 25.4 mm thick acrylic viewing plate is placed against the liquid crystal such that there is a 12.7 mm closed air gap between the liquid crystal heating foil assembly and the viewing plate. The liquid crystal can be photographed through the viewing plate.

EXPERIMENTAL ANALYSIS AND PROCEDURE

The heat transfer coefficient is calculated from the relationship

$$h = q_c/(T_w - T_{jr}) \tag{1}$$

with

$$q_c = q_e - q_l. \tag{2}$$

The energy dissipation per unit area from Joule heating is q_e. The heat loss, q_l, includes radiation and conduction (through the back of the foil). At the low jet velocities used in the present study there is little difference between the jet total temperature and the recovery temperature.

The temperature of the heating foil, T_w, is only measured at the green–blue boundary of the liquid crystal; this is the sharpest boundary observed on the liquid crystal. The temperature of this boundary, 33.3°C, is measured by inserting the liquid crystal in a water bath and determining the temperature at which the color changes green–blue and blue–green occur. The calibration was done before and after the test runs and no change occurred. In the water bath, the change in color appears to be uniform over the area of the crystal.

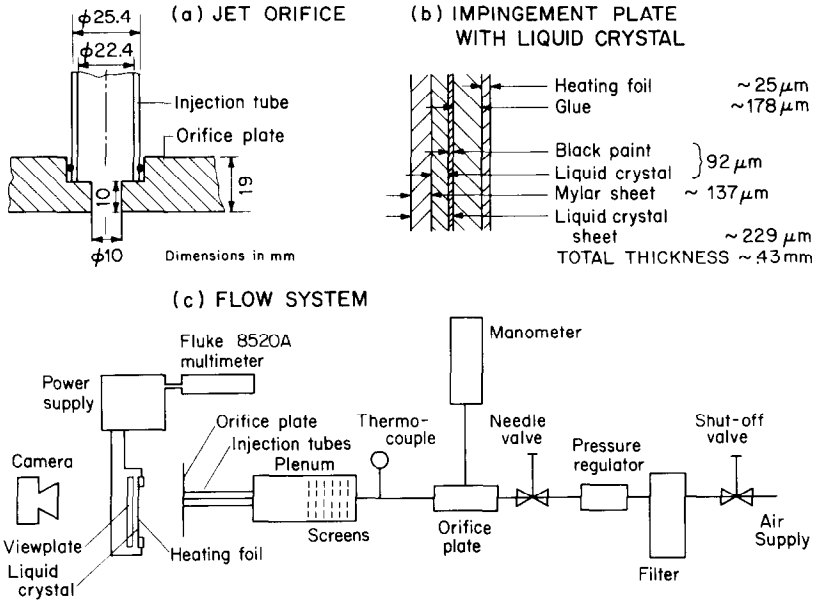

FIG. 1. Experimental apparatus.

A line of the same color (or a boundary between two colors) on the liquid crystal is related to an isotherm and if q_c is uniform to a line of constant heat transfer coefficient and constant Nusselt number. When changing the energy input by changing the current, this line will change position; it will remain the same isotherm but a different constant heat transfer coefficient line.

A series of transparencies is obtained by photographing the liquid crystal sheet through the viewing plate. Each transparency is obtained for a different heating current and thus a different q_c. Projecting the transparencies against a white paper screen and tracing the lines on a single sheet results in contours of constant Nusselt number.

For a single jet and the array of 3 co-linear jets, curves of Nusselt number vs position are obtained. To get a large number of points for the curves, the position of the isotherms is measured directly on the apparatus during a run rather than from the limited number of photographs.

Tests for each of the three jet arrays (single jet, 3 co-linear jets, and 7-jet array) were run at jet Reynolds numbers of approximately 40 000 and two different jet orifice-to-plate spacings, $L/D = 2$ and $L/D = 6$.

RESULTS

Figures 2–4 contain photographs of the liquid crystal sheet with 1, 3 and 7 jets, respectively. For each array and spacing a separate photograph was taken for each contour (frame number). The outside white–black boundaries in the pictures correspond to the green–blue boundary on the surface. In some of the photos two white–black boundaries or green–blue boundaries occur. As these both relate to the values of a given T_w and h_{gb}, they indicate a maximum or a minimum between the two similar contours.

Figure 5 shows constant Nusselt number contours at jet Reynolds number of 40 000 for two different jet-to-plate spacings ($L/D = 2$ and 6) of a single jet, the array of 3 co-linear jets, and the array of 7 jets. As indicated above, these contours are obtained by projecting the individual slides (frames) (some of which are shown in Figs. 2–4) for a given test run and tracing the green–blue boundary onto the sheet.

With the single jet at $L/D = 6$ [Fig. 5(a)], the heat transfer coefficient increases as the stagnation point is approached. This is shown in Fig. 6(a) in which the variation of the Nusselt number is plotted as measured directly on the liquid crystal sheet.

Figures 2(b), 5(b) and 6(b) show photographs of the liquid crystal, constant Nusselt number contours, and a graph of the variation of the Nusselt number with position, respectively, for a spacing $L/D = 2$. The heat transfer coefficient has a local minimum at the stagnation point (cf. ref. [1]). Apparently, the mixing-induced turbulence has not penetrated to the center of the jet because of the small spacing. The flow in the non-turbulent potential core results in a fairly small heat transfer coefficient at small R. On Frame 11 of Fig. 2(b) the 'green' band (on the picture, white) is very wide, indicating that the temperature gradient is very small. At that value of R/D (~ 2), the small variation with R in this region is also apparent in Fig. 6(a). The two outside contours have a 6-sided form [Fig. 3(b)] due to the higher flow resistance at the top and bottom of the heating foil where busbars are located.

Results for the configuration of 3 jets in a row at jet-to-plate spacing of 6 diameters are shown in Figs. 3(c), 5(c) and 7(a). The constant Nusselt number curves between the jets are flattened out and there are relative maxima between the jets (cf. refs. [1, 6, 8]). These maxima lie closer to the central jet than to the outer ones and are probably due to the higher turbulence from the interaction of the neighboring jets and the effective impingement on each other of the wall jets produced by the individual jets.

With the three co-linear jets at small spacing [Figs. 3(b), 5(d) and 7(b)], relative maxima (of the heat transfer coefficient) between the central jet and each of the two outer jets are moved away from the center jet. All the maxima are higher than at spacing $L/D = 6$. The maximum heat transfer coefficients of the outer jets do not occur at the geometric centers of the jets. The high crossflow at this small spacing causes outward movement of the maxima and the non-circular shape of the constant Nusselt curves near the outer jets. Note, again, the flattening of the constant Nu lines that occur between two jets. In contrast to a single jet at spacing $L/D = 2$, the highest heat transfer coefficient for each of the outer jets occurs at the effective stagnation point. The interference from the central jet with a strong crossflow apparently causes mixing-induced turbulence to penetrate to the jet centers for this small spacing. The center jet does have a local minimum at the stagnation point but it is less pronounced than the one for a single jet at $L/D = 2$. The potential core length would be shorter due to the interference of the neighboring jets.

With an array of 7 jets the flow is still more complex. As with the co-linear jets, the crossflow moves the location of the maximum heat transfer away from the geometric axes of the outer-jet orifices. At large spacing, $L/D = 6$ [Figs. 4(a) and 5(e)], there are relative maxima of the heat transfer coefficient between the center jet and each of the outer jets and also between each pair of outer jets. Minima in the heat transfer coefficient occur at the center of every triangle formed by 3 neighboring jet centers. Minima were found in the center of each square with a square array of jets [1].

At $L/D = 2$ [Figs. 4(b) and 5(f)], the constant Nu contours are very complex. There is a high crossflow with the large number of jets and the small spacing. The maximum heat transfer coefficients again do not coincide with the geometric centers of the outer jets. At some locations a heart-shaped contour is present [see Fig. 4(b), frames 12 and 21]. There are also maxima in heat transfer coefficient between every pair of jets and minima in the center of every triangle formed by 3 neighboring jets. Some of the individual maxima and

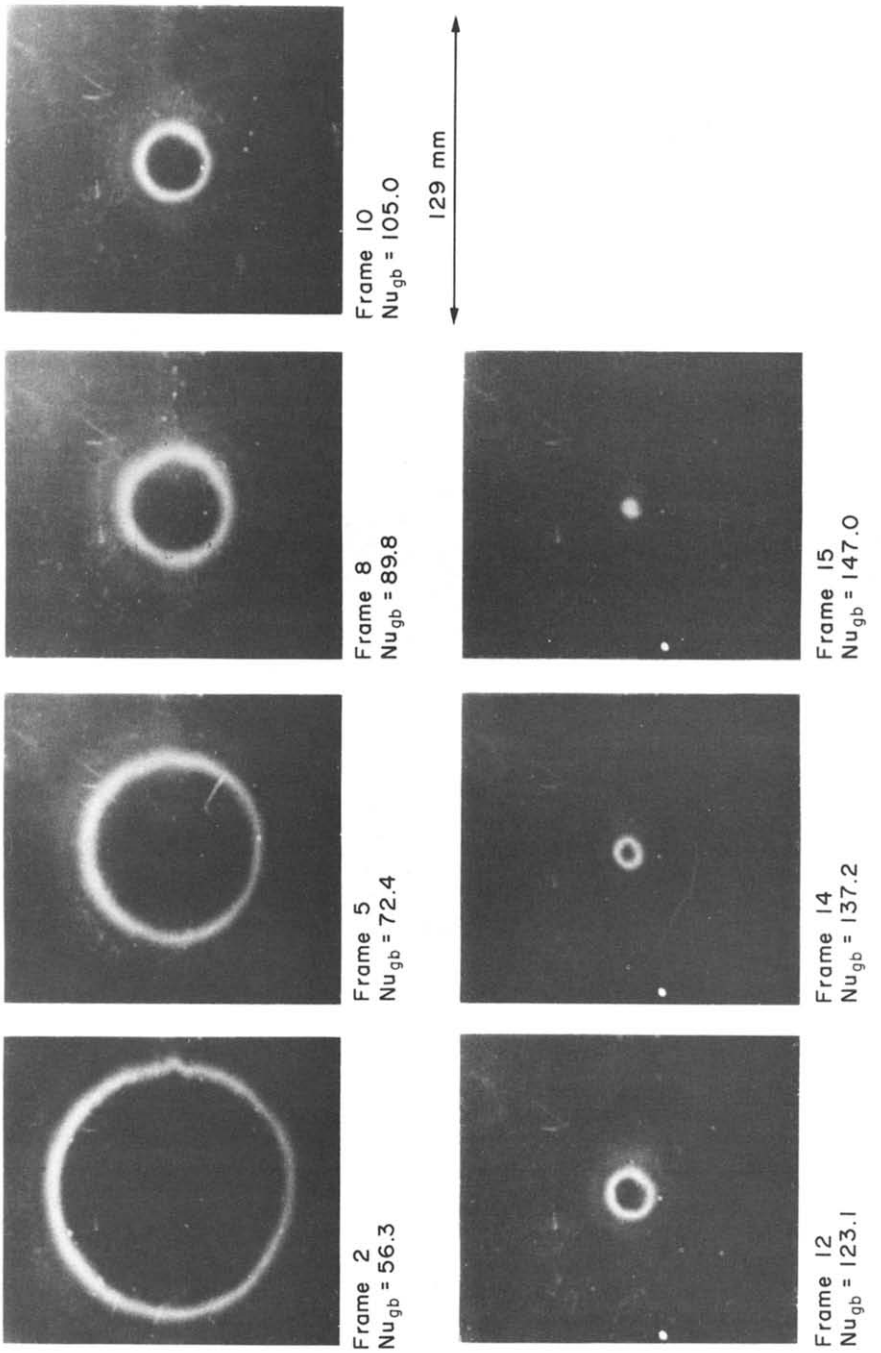

FIG. 2. Single jet impingement. Photographs of blue–green line isotherm (~ 33.3°C) on liquid crystal sheet at different heat fluxes (Nusselt numbers).

FIG. 2(a). $L/D = 6$, $Re_j = 40\,000$.

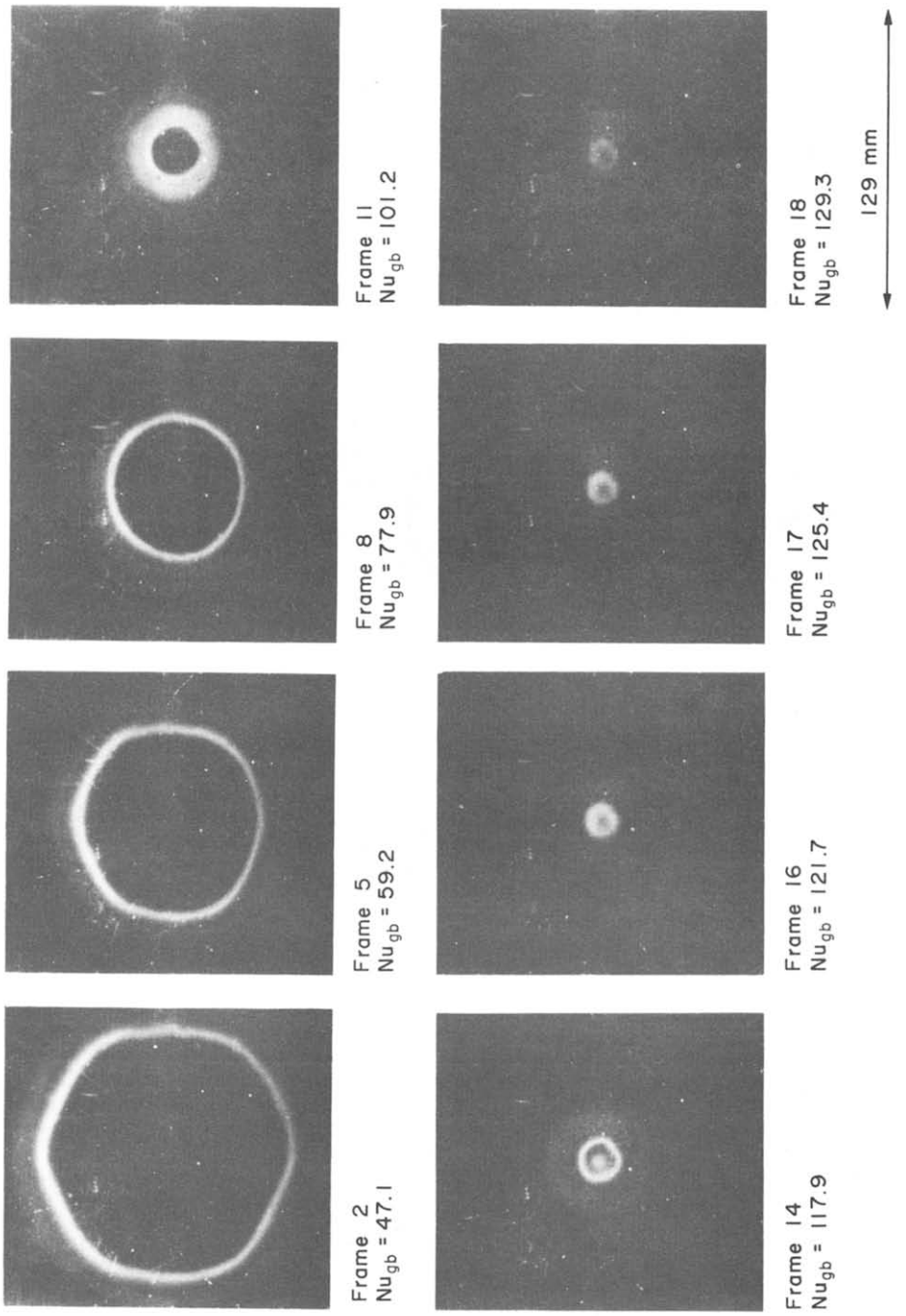

FIG. 2(b). $L/D = 2$, $Re_i = 40\,000$.

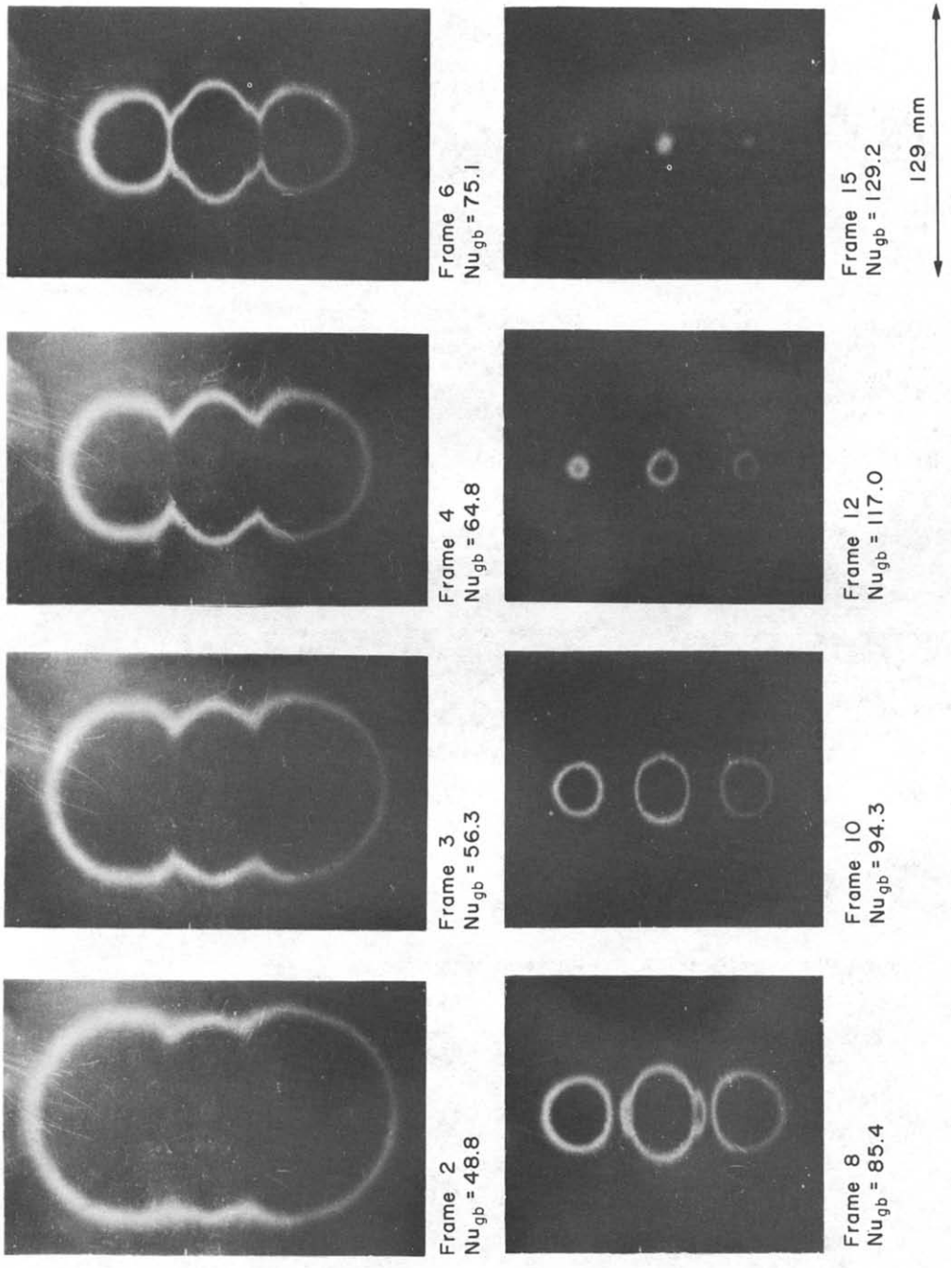

FIG. 3. Impingement from an array of three co-linear jets. Photographs of blue–green line isotherm (~33.3°C) on liquid crystal sheet at different heat fluxes (Nusselt numbers).

FIG. 3(a). $L/D = 6$, $Re_j = 40\,000$.

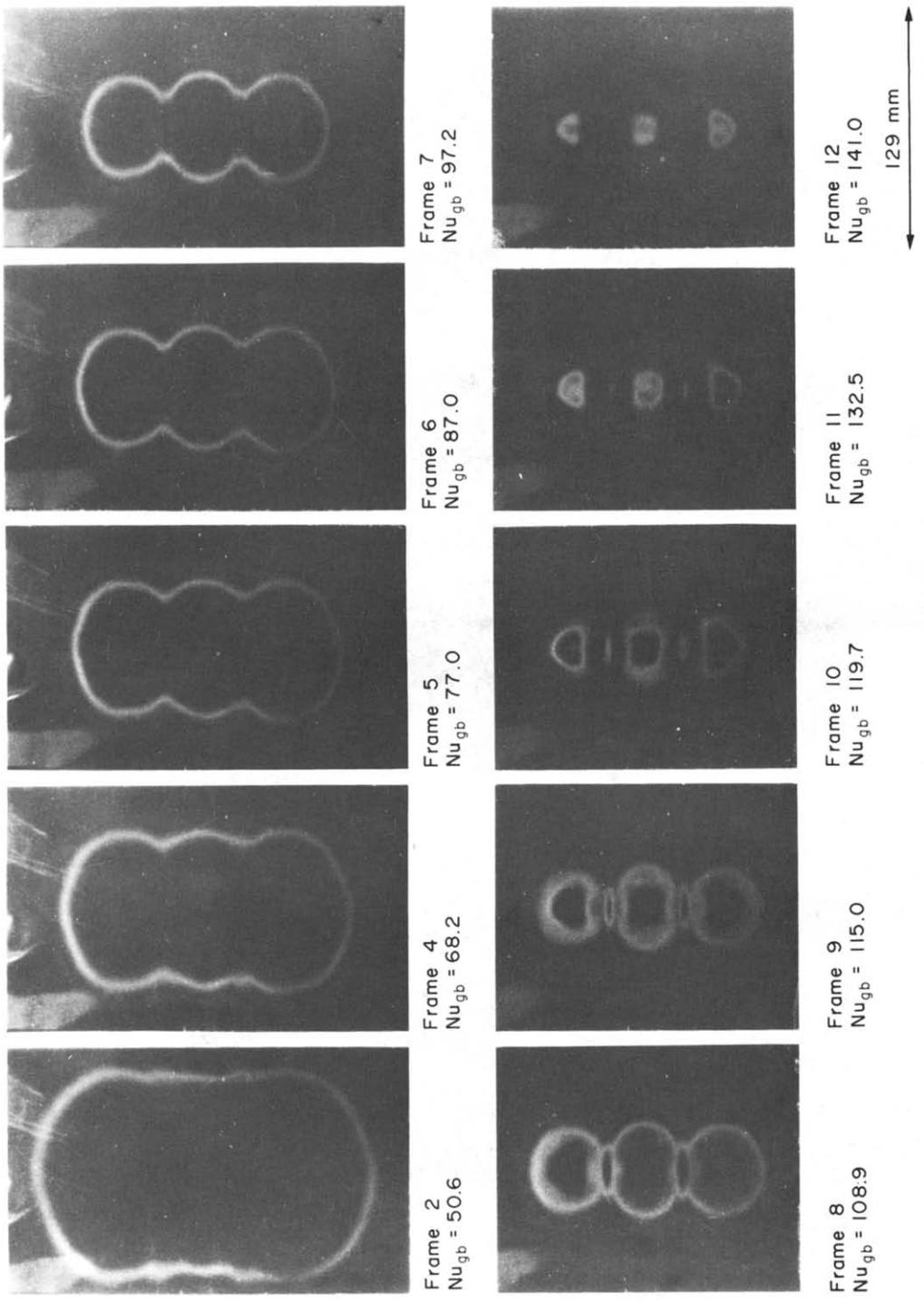

FIG. 3(b). $L/D = 2$, $Re_j = 40\,000$.

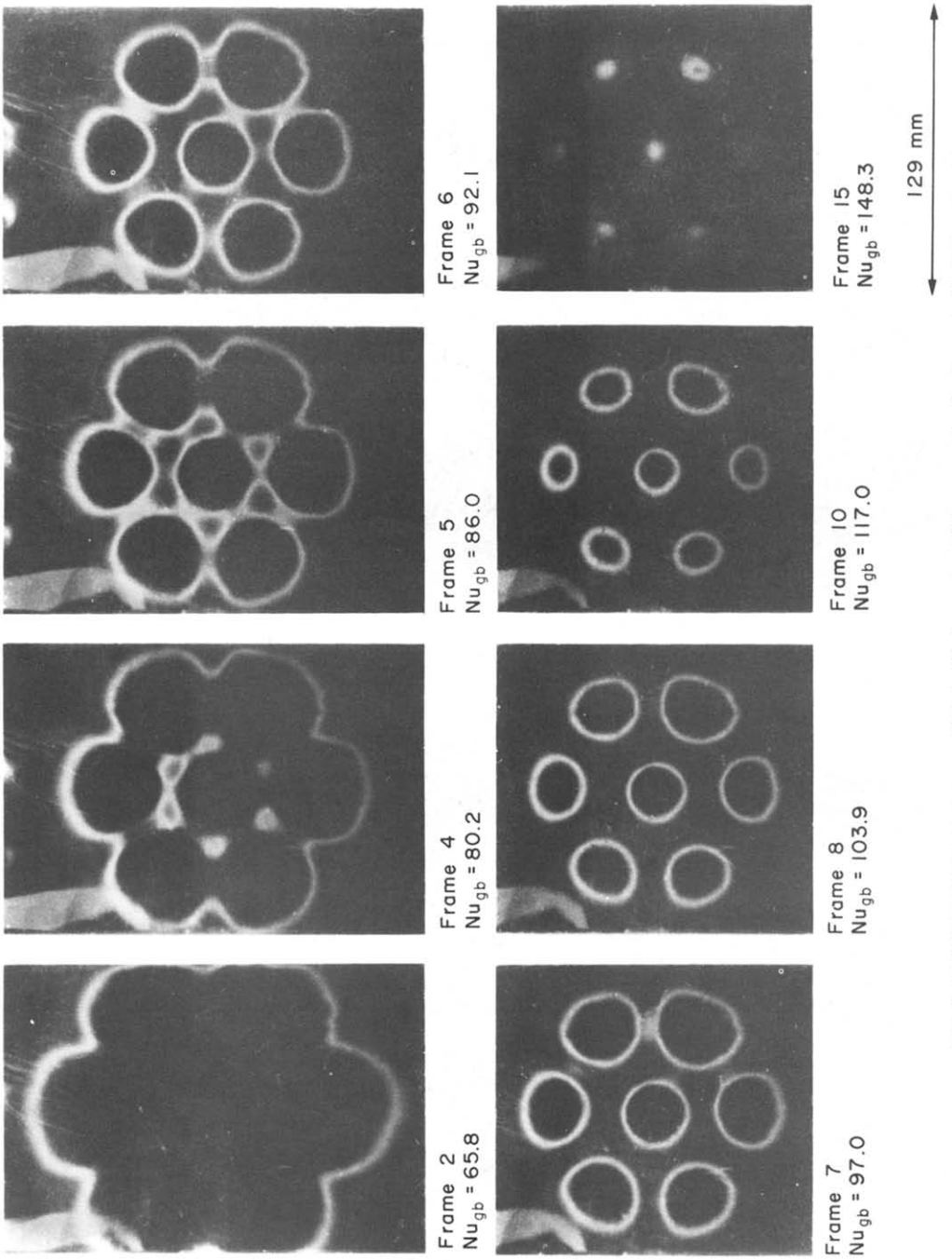

FIG. 4. Impingement from an array of 7 jets. Photographs of blue–green line isotherm (~33.3°C) on liquid cyrstal sheet at different heat fluxes (Nusselt numbers).

FIG. 4(a). $L/D = 6$, $Re_j = 40\,000$.

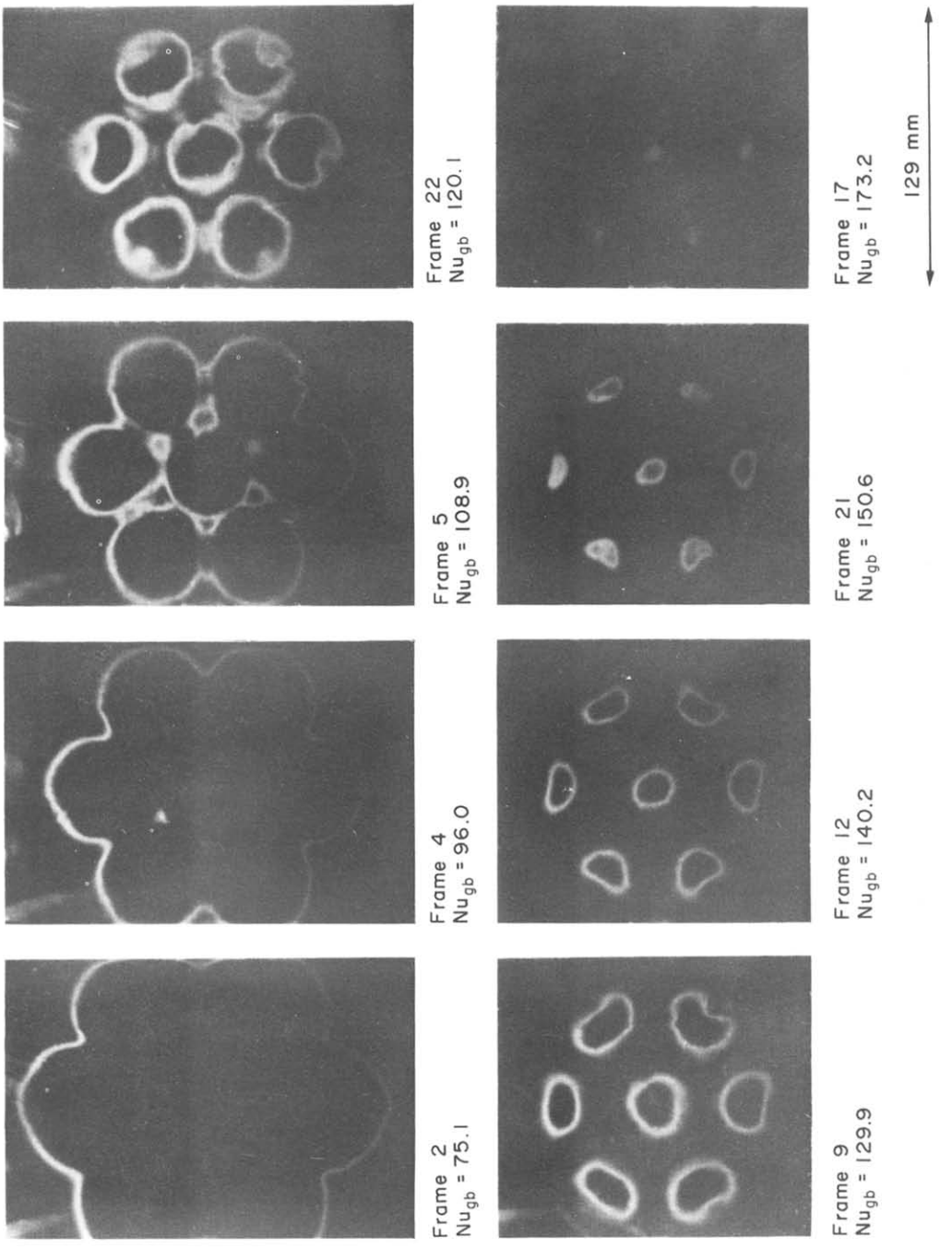

FIG. 4(b). $L/D = 2$, $Re_j = 40\,000$.

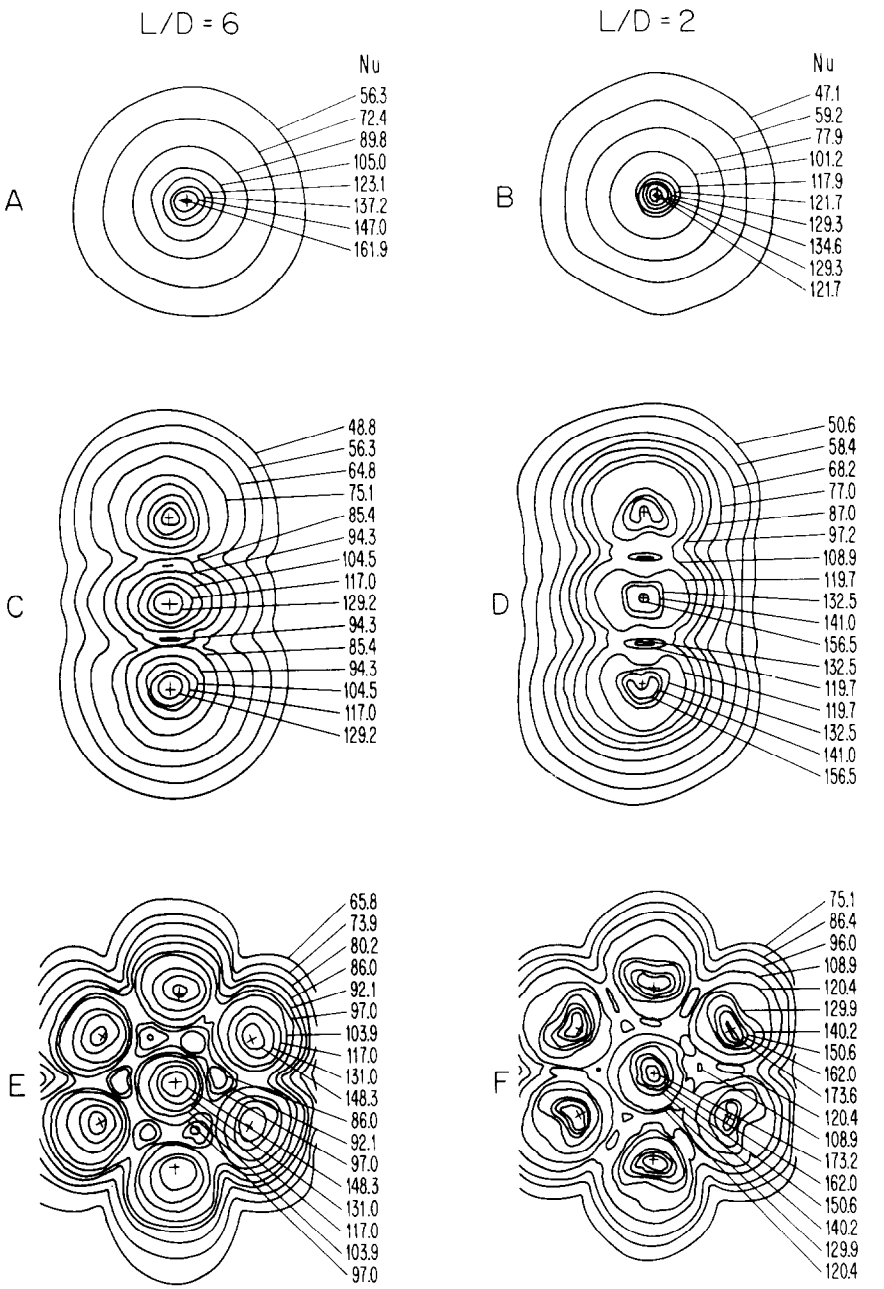

FIG. 5. Lines of constant Nusselt number for impinging heat transfer from arrays of jets.

minima are missing on the figures because the heat input was changed by discrete steps between photographs. The heat transfer coefficients are higher than those for $L/D = 6$. There are no local minima of heat transfer coefficient near the effective impingement points even with the central jet, probably due to the interference of the neighboring jets.

The stagnation point Nusselt numbers for single-jet impingement are somewhat lower than those obtained by other investigators. This is probably due to a heat gain through the air gap behind the foil and liquid crystals. Air heated behind the heating foil by the higher temperatures at large R is transported to the cooler stagnation point region. Several methods of reducing the heat transport to or from the rear of the foil were tried. These included insertion of a mesh to reduce convection and opening the region to reduce the build-up of heated air. These slightly modified the stagnation Nusselt number but had little influence on the overall heat transfer coefficient distribution.

CONCLUSIONS

A liquid crystal and a variable constant-heat-flux boundary provide a convenient system for obtaining

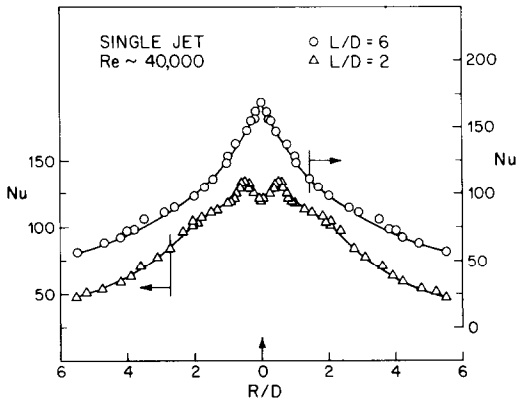

FIG. 6. Nusselt number variation with distance from geometric center of single impinging round jet.

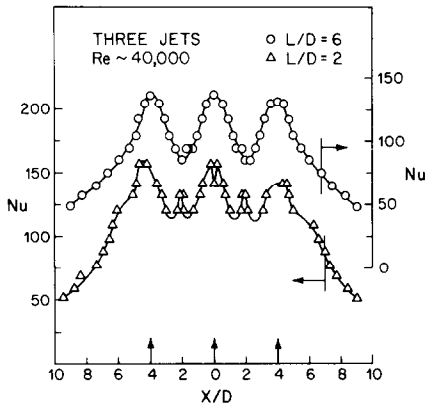

FIG. 7. Nusselt number on surface along line through geometric centers of 3-co-linear impinging jets.

qualitative and quantitative heat transfer information. Photographing the liquid crystal at different convection heat fluxes provides a series of contours of approximately constant heat transfer coefficient.

Improvement of the technique can be accomplished by finer control over the heat loss from the system which can yield a more accurate determination of the convective heat flux. For quantitative measurements it would be advantageous to use a liquid crystal whose color changes over a smaller temperature range. This, along with a monochromatic light source, could produce an even sharper isotherm.

With a single impinging jet a local minimum of Nusselt number is observed near the center of impingement for small jet-to-wall spacing ($L/D = 2$). Higher heat transfer coefficients occur at $L/D = 6$ than at $L/D = 2$. With three co-linear jets, a local minimum is observed for the central jet but not for the outer jets (at $L/D = 2$).

The outer jets in both 7-jet and 3-jet arrays are moved outward due to crossflow so that the maxima in the heat transfer coefficient from these jets occur away from the geometrical centers of the jet orifices. With these arrays, higher heat transfer coefficients occur with the smaller spacing ($L/D = 2$) than with the larger spacing ($L/D = 6$). Maxima and minima in heat transfer are also observed under some conditions in between the jets. This is particularly true at the lower jet-orifice-to-plate spacing.

With multiple jets, flow interaction can cause the mixing-induced turbulence to penetrate further towards the center of individual jets. This causes the local minimum at the stagnation point to be absent at small L/D with the array of seven jets and occur only for the center jet with the three co-linear jets.

Acknowledgements—Support from the U.S. Army Research Office under contract number ARO Proposal No. P16595-E and the Department of Energy under DOE Proposal No. DOE/DE-ACO2-81ER10810 aided in the completion of this study.

REFERENCES

1. R. Gardon and J. Cobonpue, Heat transfer between a flat plate and jets of air impinging on it, Part III, pp. 454–460. International Heat Transfer Conference Proceedings (1961).
2. R. Gardon and J. C. Akfirat, The tole of turbulence in determining the heat-transfer characteristics of impinging jets, *Int. J. Heat Mass Transfer* **8**, 1261–1272 (1965).
3. R. Gardon and J. C. Akfirat, Heat transfer characteristics of impinging two-dimensional jets, *Trans. Am. Soc. Mech. Engrs*, Series C, *J. Heat Transfer* **88**, 101–107 (1966).
4. E. U. Schlunder and V. Gnielinski, Warme-und Stoffubertragung zwischen gut und aufprallende Dusenstrahl, *Chem. Ing. Tech.* **39**, 578–584 (1967).
5. C. den Ouden and C. J. Hoogendoorn, Local convective heat transfer coefficients for jets impinging on a flat plate; experiments using a liquid crystal technique, in *Heat Transfer 1974 (Proc. 5th Int. Heat Transfer Conf., Tokyo)*, Vol. 5, pp. 293–297. Tokyo: The Japan Society of Mechanical Engineers/The Society of Chemical Engineers (1974).
6. R. N. Koopman, Local and average transfer coefficients for multiple impinging jets, Ph.D. Thesis, Department of Mechanical Engineering, University of Minnesota (1975).
7. D. E. Metzger, D. I. Florshuetz, R. Takeuchi, D. Behee and R. A. Berry, Heat transfer characteristics for inline and staggered arrays of circular jets with crossflow of spent air, *Trans. Am. Soc. Mech. Engrs*, Series C, *J. Heat Transfer* **101**, 526–531 (1979).
8. A. I. Behbahani, Heat transfer to staggered arrays of impinging circular jets, Ph.D. Thesis, Department of Mechanical Engineering, University of Minnesota (1979).
9. T. Raad and J. E. Myers, Nucleation studies in pool-boiling on thin plates using liquid crystals, *A.I.Ch.E. J* **15**, 1260–1261 (1971).
10. T. E. Cooper and W. K. Petrovic, An experimental investigation of the temperature fields produced by a surgical cannula, *Trans. Am. Soc. Mech. Engrs*, Serie C, *J. Heat Transfer* **96**, 415–420 (1974).
11. M. Hirata, N. Kasagi and M. Kumada, Studies of full-coverage film-cooling, 1980 *U.S.–Japan Joint Heat Transfer Conf., Tokyo*, Japan, 28 September–2 October 1980, to be published.
12. E. J. Klein, Liquid crystals in aerodynamic testing, *Astronautics and Aeronautics* **6**, 70–73 (1968).
13. T. E. Cooper, R. J. Field and J. F. Meyer, Liquid crystal thermography and its application to the study of convective heat transfer, *Trans. Am. Soc. Mech. Engrs*, Series C, *J. Heat Transfer* **97**, 442–450 (1975).
14. G. W. Gray, *Molecular Structure and the Properties of*

Liquid Crystals. Academic Press, London (1962).
15. J. L. Ferguson, Liquid crystals in non-destructive testing, *Appl. Optics* **7**, 1729–1737 (1968).
16. R. E. Engelhardt and W. A. Hewglen, Thermal and infrared testing in non-destructive testing, NASA Report SP-5113 (1973).

VISUALISATION DU TRANSFERT THERMIQUE PAR DES LIGNES DE JETS INCIDENTS

Résumé—Une technique de visualisation est utilisée pour mesurer la distribution du coefficient de transfert thermique sur une plaque plane frappée par un jet unique ou par une ligne de jets. Des cristaux liquides sur une feuille de mylar sont utilisés pour localiser les isothermes sur la surface chauffée. En ajustant le flux surfacique de chaleur, on obtient les contours du coefficient constant de transfert thermique.

SICHTBARMACHUNG DES WÄRMEÜBERGANGS VON FELDERN SENKRECHT AUFTREFFENDER STRAHLEN

Zusammenfassung—Eine Sichtbarmachungs-Methode wird benutzt, um die Verteilung des Wärmeübergangskoeffizienten auf einer ebenen Platte zu bestimmen, auf welche entweder ein einzelner Strahl oder ein Feld von Strahlen senkrecht aufrifft. Flüssigkristalle, auf eine Mylar-Folie aufgebracht, werden verwendet, um den Isothermenverlauf auf einer beheizten Oberfläche zu bestimmen. Durch Einstellen der Wärmestromdichte an der Oberfläche lassen sich Konturen konstanter Wärmeübergangskoeffizienten gewinnen.

ВИЗУАЛИЗАЦИЯ ПРОЦЕССА ТЕПЛООТДАЧИ СИСТЕМ ИМПАКТНЫХ СТРУЙ

Аннотация—Метод визуализации используется для измерения распределения коэффициента теплоотдачи на плоской пластине, на которую падает единичная струя или система струй. Для определения положения изотерм на нагреваемой поверхности использовалась пластина из майлара с жидкокристаллическим покрытием. Путем соответствующего выбора величины теплового потока на поверхности получены линии постоянного коэффициента теплоотдачи.